Microscopic description of the beta delayed deuteron emission from ^{6}He

Attila Csótó[1,2,*] and Daniel Baye [1]
[1] *Physique Nucléaire Théorique et Physique Mathématique, C.P. 229, Campus Plaine, Université Libre de Bruxelles, B-1050 Brussels, Belgium*
[2] *Institute of Nuclear Research of the Hungarian Academy of Sciences P.O.Box 51 Debrecen, H-4001, Hungary*
(Received 1 October 1993)

The beta delayed deuteron emission from ^{6}He is studied in a dynamical microscopic cluster model. This model gives a reasonably good description for all the subsystems of ^{6}He and ^{6}Li in a coherent way, without any free parameter. The beta decay transition probability to the ^{6}Li ground state is underestimated by a few percent. The theoretical beta delayed deuteron spectrum is close to experiment but it is also underestimated, by about a factor of 1.7. We argue that, in spite of their different magnitudes, both underestimations might have a common origin. The model confirms that the neutron halo part of the ^{6}He wave function plays a crucial role in quenching the beta decay toward the $\alpha + d$ channel.

PACS number(s): 23.40.Hc, 21.60.Gx, 27.20.+n

I. INTRODUCTION

In the past few years the large amount of experimental data which have been accumulated on the structure and reactions of unstable nuclei revealed the existence of a neutron halo structure in nuclei with a large neutron excess [1,2]. The best known of these nuclei is ^{11}Li. However, there are ambiguities in the theoretical description of this nucleus mainly because few ^{9}Li $+n$ scattering data are available, and because the ^{9}Li core is soft [3]. Fortunately, these problems do not occur in the case of the other prominent neutron halo nucleus, ^{6}He. Sophisticated calculations exist which can account for several properties of ^{6}He [3–7].

One of the most surprising features of ^{6}He is the very small Gamow-Teller (GT) beta decay branching ratio toward the $\alpha + d$ continuum channel. The β delayed deuteron emission from ^{6}He was first observed in Ref. [8], and the measured branching ratio $(2.5 \pm 0.5) \times 10^{-6}$ is two orders of magnitude smaller than the result of a phenomenological analysis of the decay process in terms of an R-matrix formalism [8]. Later an experiment with higher statistics resulted in a new value $(7.6 \pm 0.6) \times 10^{-6}$ [9]. Even this larger value is overestimated in a potential model [10] and in a three-body $\alpha + n + n$ model [11].

A semimicroscopic model [12] shows that the smallness of the branching ratio is the result of a cancellation, taking place between two parts of the GT matrix element, which have different signs. The "internal" part comes from the typical nuclear regions ($r < 5$ fm) of the ^{6}He and $\alpha + d$ wave functions. The "external" part comes from the 5 fm $< r <$ 20 fm region. The importance of the latter part is a clear consequence of the halo structure in ^{6}He. In that semimicroscopic model, the ^{6}He initial state is described with a six-nucleon microscopic wave function but the final state is treated in a potential model. This hybrid treatment is flexible enough to reveal the quenching mechanism of the branching ratio. However, its agreement with experiment is probably partly fortuitous because the results are very sensitive to model assumptions. In Ref. [10] the branching ratio is overestimated by an order of magnitude because the assumption of a pure α + dineutron configuration enhances the "external" part of the GT matrix element. In Ref. [11] the overestimation is reduced because of a much more realistic description of ^{6}He but the treatment of the $\alpha + d$ scattering state is not consistent with the treatment of the ^{6}He ground state.

Clearly, an accurate and consistent description of this process is desirable. However, obtaining reliable results requires that the following conditions are met. The model must reproduce in a realistic way (i) the deuteron binding energy and size, (ii) the low-energy $n + n$ phase shifts, (iii) the $\alpha + n$ scattering, (iv) the $\alpha + d$ scattering, and (v) the ^{6}He binding energy and size. In addition the analysis of Ref. [12] indicates that (vi) the halo must be well described up to distances as large as 20 fm. In this paper we calculate the β delayed deuteron spectrum in a fully microscopic model. We try to use a parameter free model without any *ad hoc* model assumption. With the Minnesota interaction conditions (i)–(iv) are fulfilled [13,14] and a good ^{6}He wave function satisfying (v) is available [7] although the basis has to be enlarged to meet (vi). The fact that a few percent error in the model at typical nuclear scales can modify the order of magnitude of the final result, as is pointed out in Ref. [12], calls for a test example which is sensitive to the details of the wave functions only up to less than 10 fm. Our test case will be the β decay transition to the ground state of ^{6}Li.

The model is recalled in Sec. II. The results are described and discussed in Sec. III. Conclusions are presented in Sec. IV.

*Electronic address: H988CSO@HUELLA.BITNET

II. MODEL

The β delayed deuteron emission probability per time and energy units, dW/dE, can be expressed [15,12] as

$$\frac{dW}{dE} = \frac{mc^2}{\pi^4 v\hbar^4} G_\beta^2 f(Q-E) B_{\rm GT}(E), \tag{1}$$

where m is the electron mass, v is the relative velocity between α and deuteron, and $G_\beta = 3.002 \times 10^{-12}$ is the dimensionless β decay constant. The phase space factor, or Fermi integral, f depends on the kinetic energy $Q-E$ available for the electron and antineutrino. The mass difference Q between the initial and final particles is 2.03 MeV. The maximum total energy (including mass energy) is $W_0 = 2.54$ MeV. The GT reduced transition probability reads

$$B_{\rm GT}(E) = \frac{\lambda^2}{2J+1} \sum_{MM'\mu} |\langle \Psi^{\alpha d}_{J'M'} \mid \sum_{j=1}^{6} t^j_- \sigma^j_\mu \mid \Psi^{^6{\rm He}}_{JM} \rangle|^2, \tag{2}$$

where $\Psi^{\alpha d}$ and $\Psi^{^6{\rm He}}$ are the microscopic wave functions of the $\alpha+d$ scattering state and of the ^{6}He ground state, respectively (we shall specify them later), $\boldsymbol{t}^j$ and $\boldsymbol{\sigma}^j$ are respectively the isospin operator and Pauli spin matrices of nucleon j, and $\lambda = 1.26$ is the ratio of the axial-vector to vector coupling constants. The half-life $t_{1/2}$ for the β decay to the ground state of ^{6}Li is calculated with

$$(ft_{1/2})^{-1} = (2\ln 2)\pi^3 (mc^2/\hbar) G_\beta^2 B_{\rm GT}({\rm g.s.}), \tag{3}$$

where $B_{\rm GT}$(g.s.) is given by

$$B_{\rm GT}({\rm g.s.}) = \frac{\lambda^2}{2J+1} \sum_{MM'\mu} |\langle \Psi^{^6{\rm Li}}_{J'M'} \mid \sum_{j=1}^{6} t^j_- \sigma^j_\mu \mid \Psi^{^6{\rm He}}_{JM} \rangle|^2. \tag{4}$$

In Ref. [7] a microscopic dynamical model has been developed for the description of the ground state of ^{6}He. In the present work we use the wave function of that model

$$\begin{aligned}
\Psi^{^6{\rm He}}_{JM} &= \sum_{S,l_1,l_2,L} \Psi^{\alpha(nn)}_{S,(l_1l_2)L} + \sum_{S,l_1,l_2,L} \Psi^{n(\alpha n)}_{S,(l_1l_2)L} + \Psi^{tt}_{S,L} \\
&= \sum_{S,l_1,l_2,L} \sum_{i=0}^{N_a-1} \mathcal{A}\left\{ \left[[\Phi^\alpha_i (\Phi^n \Phi^n)]_S \chi^{\alpha(nn)}_{i[l_1l_2]L}(\boldsymbol{\rho}_{nn}, \boldsymbol{\rho}_{\alpha(nn)}) \right]_{JM} \right\} \\
&+ \sum_{S,l_1,l_2,L} \sum_{i=0}^{N_a-1} \mathcal{A}\left\{ \left[[\Phi^n (\Phi^\alpha_i \Phi^n)]_S \chi^{n(\alpha n)}_{i[l_1l_2]L}(\boldsymbol{\rho}_{\alpha n}, \boldsymbol{\rho}_{n(\alpha n)}) \right]_{JM} \right\} \\
&+ \sum_{S,L} \mathcal{A}\left\{ \left[[\Phi^t \Phi^t]_S \chi^{tt}_L(\boldsymbol{\rho}_{tt}) \right]_{JM} \right\}.
\end{aligned} \tag{5}$$

Here $\mathcal{A}$ is the intercluster antisymmetrizer, the $\boldsymbol{\rho}$ vectors are the different intercluster Jacobi coordinates, and [ ] denotes angular momentum coupling. While Φ^n is a neutron spin-isospin eigenstate, Φ^t is the antisymmetrized triton internal state in the harmonic oscillator shell-model with a single oscillator parameter. The antisymmetrized ground state ($i=0$) and monopole excited states ($i>0$) of the α particle are represented by the wave functions

$$\Phi^\alpha_i = \sum_{j=1}^{N_a} A_{ij} \phi^\alpha_{\beta_j}, \quad i = 0, 1, ..., (N_a - 1), \tag{6}$$

where $\phi^\alpha_{\beta_j}$ is a translation invariant shell–model wave function of the α particle with size parameter β_j and the A_{ij} parameters are to be determined by minimizing the energy of the α particle [16]. Similarly the size parameter of the tritons is determined from the energy stabilization. We choose the same parameters for the wave function as in Ref. [7] with $N_a = 3$. The following SL terms are included in the $S,(l_1l_2)L$ coupling scheme for the $J^\pi = 0^+$ ground state of ^{6}He: $\{\alpha(nn);0(00)0\}$, $\{\alpha(nn);1(11)1\}$, $\{n(\alpha n);0(00)0\}$, $\{n(\alpha n);0(11)0\}$, $\{n(\alpha n);1(11)1\}$, and $\{tt,00\}$. Putting (5) into the six-nucleon Schrödinger equation, we arrive at an equation for the intercluster relative motion functions χ. These functions are expanded in terms of products of tempered Gaussian functions $\exp(-\gamma_i \rho^2)$ [17] with different ranges γ_i for each type of relative coordinate. The expansion coefficients are determined from a variational principle.

The Minnesota force [13] with an exchange parameter $u = 0.92$ and a slightly modified spin-orbit component (see Ref. [7]) reproduces very well the experimental phase shifts of all the $N+N$ and $\alpha+N$ scattering states which take place in (5) [7]. After this force choice there remains no free parameter in the model. This model gives for ^{6}He an $\alpha+n+n$ three-cluster separation energy of 0.961 MeV, i.e., practically the experimental value 0.975 MeV. It was pointed out in Ref. [7] that this value could not be reproduced without the $t+t$ component. As the GT matrix element is sensitive to the details of the ^{6}He wave function up to 15–20 fm in the $\rho_{\alpha(nn)}$ coordinate [12], our wave function should be correct in this region. To achieve this, we enlarge the number of basis states which describe large $\rho_{\alpha(nn)}$ separations in such a way that the range of our last basis functions is $\sim$ 20 fm in these relative motions.

To be consistent, we must employ the same model parameters in the description of the $\alpha+d$ bound and scattering states as for ^{6}He. For example, the use of a differ-

ent nucleon-nucleon interaction for $\alpha+d$ would affect the product of the spatial parts of the ^{6}He and $\alpha + d$ wave functions and modify the balance between the different parts in the GT matrix element, and could lead to inaccurate results. The Minnesota force reproduces the $N+N$ effective range parameters in the triplet even partial wave by assuming a pure $^3S_1$ state, i.e., without tensor coupling with a D state. However, if a tensor force were taken into account in addition to the Minnesota force, it would play a very large role in this partial wave in a coupled $^3S_1$-$^3D_1$ description [18]. This means that if a pure $^3S_1$ state reproduces the experiment, then the effective interaction in this partial wave is too strong. As was pointed out in [7], the Minnesota interaction overbinds the ground state of ^{6}Li by 1.2 MeV when all possible angular momentum configurations are taken into account. To avoid this, we keep only the $L=0$, $S=1$ configuration. The error we make with this truncation is acceptable because only a $\sim 5\%$ $L \neq 0$ component [19] in ^{6}Li is neglected, but in compensation the asymptotic form of the wave function is more realistic. The contribution to $B_{\rm GT}$ from the ^{6}He ($L=1$)$\rightarrow^6$Li transition would be negligible ($\sim 0.1\%$) since the GT operator only connects states with the same L. However, because of the lack of the $L=1$ component, the weight of the $L=0$ component is increased so that $B_{\rm GT}$ might be overestimated by 5% although the variational principle might partly compensate this effect. Also the presence of $L \neq 0$ components in the ^{6}Li wave function might slightly shift the positions of its nodes. The importance of these errors can be estimated from the calculation of $B_{\rm GT}$(g.s.).

After these choices, our ^{6}Li wave functions read with $L=0$, $S=1$, and $J^\pi = 1^+$,

$$\Psi^{^6{\rm Li}}_{JM} = \sum_{i=0}^{N_d-1} \mathcal{A}\left\{\left[[\Phi^\alpha \Phi^d_i]_S\, \chi^{\alpha d}_{iL}(\boldsymbol{\rho}_{\alpha d})\right]_{JM}\right\} + \mathcal{A}\left\{\left[[\Phi^t \Phi^h]_S\, \chi^{th}_L(\boldsymbol{\rho}_{th})\right]_{JM}\right\} \quad (7)$$

for the ground state, and

$$\Psi^{\alpha d}_{JM} = \mathcal{A}\left\{\left[[\Phi^\alpha \Phi^d_0]_S\, g^{\alpha d}_L(E,\boldsymbol{\rho}_{\alpha d})\right]_{JM}\right\} + \sum_{i=1}^{N_d-1} \mathcal{A}\left\{\left[[\Phi^\alpha \Phi^d_i]_S\, \chi^{\alpha d}_{iL}(E,\boldsymbol{\rho}_{\alpha d})\right]_{JM}\right\} + \mathcal{A}\left\{\left[[\Phi^t \Phi^h]_S\, \chi^{th}_L(E,\boldsymbol{\rho}_{th})\right]_{JM}\right\} \quad (8)$$

for the scattering states ($h=^3$He), where E is the $\alpha+d$ relative motion energy in the center-of-mass frame. The normalization of g is chosen consistently with (3) as

$$g^{\alpha d}_0(E,\boldsymbol{\rho}_{\alpha d}) \rightarrow Y_{00}(\hat{\boldsymbol{\rho}}_{\alpha d})\rho^{-1}_{\alpha d} \times \Big(F_0(k\rho_{\alpha d})\cos\delta + G_0(k\rho_{\alpha d})\sin\delta\Big) \quad (9)$$

if $\rho_{\alpha d} \rightarrow \infty$, where k is the wave number, F_0 and G_0 are Coulomb functions, and δ is the s-wave phase shift, at energy E.

The deuteron cluster being very distortable we use five basis states ($N_d = 5$) for its description. The ground state Φ^d_0 with -2.20 MeV energy and 2.1 fm (point nucleon) rms radius, and four pseudostates Φ^d_i, are included in (7) and (8). Because the distortion of the α particle is weak in scattering processes, we describe it with a single stabilized size parameter. Using the same force as for ^{6}He, the ground state of ^{6}Li described by (7) provides the experimental $\alpha + d$ cluster separation energy of 1.47 MeV. It is remarkable that we can reproduce both the ^{6}Li and ^{6}He ground states with the same force in this model. Notice that other configuration choices underestimate the binding energy. (i) Without the t+^{3}He component, ^{6}Li is underbound by more than 0.5 MeV. (ii) This result is *not* improved by α distortion. (iii) With α distortion *and* the t + ^{3}He component, ^{6}Li is also underbound but by the smaller value 0.24 MeV; the role of t+^{3}He is weakened because of a higher threshold. For the purpose of tests described below, it is interesting to have another wave function reproducing the experimental ^{6}Li energy without the t+^{3}He component. This can be achieved by refitting the exchange mixture parameter to the value $u = 0.97$.

The scattering states are calculated from a Kohn-Hulthén variational method for the S matrix, which uses square integrable basis functions matched with the correct scattering asymptotics [17]. To make the calculations numerically stable, the matching radius must be chosen in the 10–15 fm region. In order to calculate $B_{\rm GT}$ analytically up to 25–30 fm, the scattering wave function g coming from the variational method is also expanded in terms of square integrable tempered Gaussian functions. The squared deviation between g and this expansion is variationally minimized up to 40 fm and becomes less than 10^{-8}. The $L=0$ $\alpha + d$ phase shifts in the $E = 0.1 - 5.0$ MeV relative center-of-mass energy region are compared with experiment [20] in Fig. 1. They agree within 0.1° with those obtained with the potential of Ref. [21], which is fitted to experiment. Putting the $\Psi^{^6{\rm He}}$, $\Psi^{^6{\rm Li}}$, and $\Psi^{\alpha d}(E)$ wave functions, coming from the variational calculations, into (2) and (4) we can compute the desired $B_{\rm GT}$ and $B_{\rm GT}$(g.s.) matrix elements. All calculations are performed analytically by the aid of a symbolic computer language.

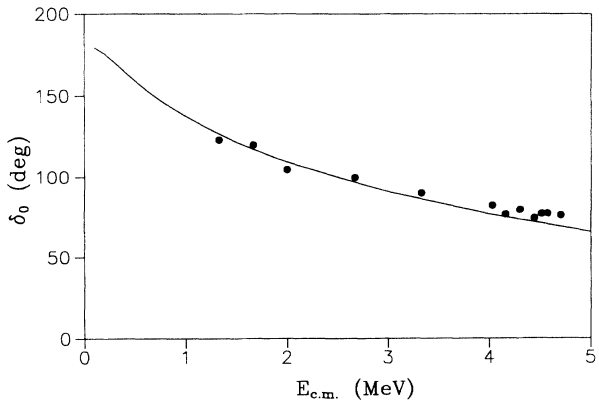

FIG. 1. $\alpha + d$ phase shift for the s wave obtained with the microscopic wave function $\Psi^{\alpha d}_{JM}$ [Eq. (8)]. The experimental points are taken from [20].

Comparing our model to the previous theoretical models [10–12] we can say the following. A common drawback of those three models is that the $\alpha + d$ scattering states are obtained from an $\alpha + d$ nucleus-nucleus potential. Although this nonmicroscopic potential model reproduces the correct $\alpha + d$ phase shifts, the inner part of the scattering wave functions is not well established. It may not be consistent with the ^{6}He description. In Ref. [10], ^{6}He is represented by a pure $\alpha(nn)$ configuration. The dineutron component is therefore overestimated in the ^{6}He wave function, and hence in its halo part. Consequently, the external part of the GT matrix element and $B_{\rm GT}$ are too large. In Ref. [11], the results are rather insensitive to the use of an attractive or a repulsive interaction in the s wave, which both reproduce the phase shifts. This insensitivity is rather surprising because phase-equivalent potentials usually do not lead to the same results for off-shell effects [22]. As we can see, e.g., in Fig. 3 of Ref. [11], the repulsive potential does not produce an internal node in the $\alpha + d$ wave function, while the attractive potential produces such a node (Fig. 2 of Ref. [10]). Therefore, the GT matrix elements with the ^{6}He wave function should be very different from each other. This effect is probably hidden by the orthogonalization procedure adopted by the authors of Ref. [11]. In Ref. [12], the ^{6}He wave function is not totally free for the variational method: In the halo, the spatial part is restricted to small interneutron distances. As the interaction, employed there, does not reproduce correctly the $n + n$ scattering and binds the dineutron, it might distort the halo in a larger variational space. Moreover neglecting the $\sim 15\%$ $L \neq 0$ component in that wave function leads to an enlargement of $B_{\rm GT}$. Finally, using a microscopic wave function as initial state with an $\alpha + d$ potential wave function as final state, even with the correct phase shifts, is not consistent. The present model is essentially free of such defects. The description of ^{6}He is consistent with that of ^{6}Li and of $\alpha + d$, the interaction satisfies conditions (i)–(vi) of Sec. I and does not bind the dineutron, and $L \neq 0$ components are explicitly included in the description of ^{6}He.

III. RESULTS AND DISCUSSION

For $B_{\rm GT}$(g.s.) we obtain $4.60\lambda^2$ in our model which corresponds to $ft_{1/2} = 841$ ms or a half-life $t_{1/2} \approx 835$ ms, to be compared with the experimental value $t_{1/2} = 806.7 \pm 1.5$ ms [23]. In the test model, where the t+^{3}He component is omitted in ^{6}Li and the force is refitted, we get $4.48\lambda^2$ for $B_{\rm GT}$(g.s.) and 857 ms for $t_{1/2}$. This example shows the importance of using the same interaction in both the initial and final states of the decay process: The error on the theoretical result is doubled in the test calculation. The 3–4% deviation from experiment in the full model can be considered as a good agreement. Of course the lack of $L = 1$ component in ^{6}Li probably reduces the difference between theory and experiment. Nevertheless, as discussed in Ref. [5], deviations as large as 7–8% could be accounted for by meson-exchange current corrections. Corrections of this size are typical of different weak processes in few-nucleon systems (see, e.g., Ref. [24]).

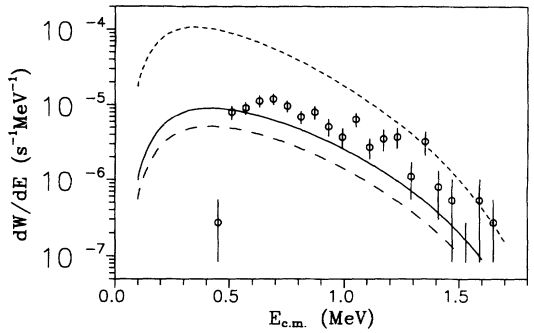

FIG. 2. Transition probability dW/dE per time and energy units in the center-of-mass frame as a function of the center-of-mass energy E. The experimental points are taken from Ref. [9], while the statistical error bars are from Ref. [12]. The solid curve is the result of the present calculation with the t+^{3}He component included in the $\alpha + d$ wave function, while the long-dashed curve is the result without this component. The short-dashed curve is obtained by dropping the $\rho_{\alpha(nn)} > 10$ fm part of the full ^{6}He wave function.

The calculated dW/dE curves are shown in Fig. 2 together with the experimental points of Ref. [9]. We can see that both the full, consistent, model (solid curve) and the test model (long-dashed curve) undershoot the experimental points, but the results of the consistent model are much closer to them. As for $B_{\rm GT}$(g.s.), the deviation from experiment is roughly twice as large in the test model as in the full one. The error on $B_{\rm GT}$(g.s.) is typical of a process occurring at the normal nuclear scale, i.e., at usual distances between nucleons in a nucleus. This factor of 2 is still observed in dW/dE. However, the 3–4% error on $B_{\rm GT}$(g.s.) in our best model is amplified to 60–70% on dW/dE. This emphasizes again that the small $B_{\rm GT}$ value in the β decay to $\alpha + d$ is the result of a balanced cancellation between two larger values with different signs. The total branching ratio in the consistent model is 6.0×10^{-6}. The branching ratio for deuterons whose energy is above the experimental cutoff [9] is 3.1×10^{-6}. Let us note that the integration of the experimental data in Fig. 2 provides 5.4×10^{-6}, i.e., less than the value $(7.6 \pm 0.6) \times 10^{-6}$ quoted in Ref. [9].

To seek further after possible origins of errors, we changed the number of basis functions between 8 and 25 in the critical region of $\alpha(nn)$ relative motion in ^{6}He, each basis always ensuring the covering of this region up to 20–25 fm. Our results remain stable within one percent. Next we checked the asymptotics of our ^{6}He wave function. In Fig. 3 we show the radial part of the $\chi^{\alpha(nn)}_{0[00]0}$ relative motion function at fixed $\rho_{nn} = 2$ fm. One can see that the Gaussian cutoff starts only at roughly 30 fm. The correct asymptotic behavior of the bound state wave function of three neutral particles which have no bound binary subchannels is given by [25]

$$\Psi \to \varrho^{-5/2} \exp(-\kappa\varrho) \qquad (10)$$

if $\varrho \to \infty$. Here ϱ is the hyperradius (defined by $\varrho^2 =$

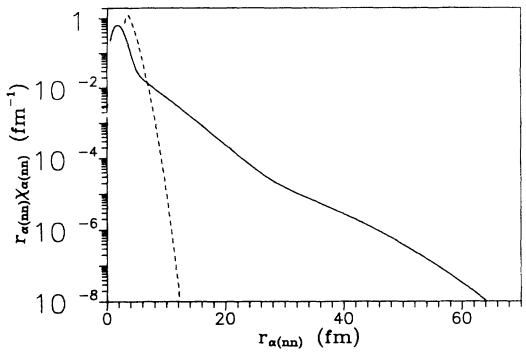

FIG. 3. Radial part of the $\chi^{\alpha(nn)}_{0[00]0}$ relative motion function of the ^{6}He wave function (full line) calculated for $\rho_{nn} = 2$ fm, and its truncated approximation (short-dashed curve) corresponding to the short-dashed curve in Fig. 2.

$\sum_i A_i r_i^2$, where $\boldsymbol{r}_i$ is the center-of-mass coordinate of cluster i with respect to the center of mass of the three-cluster system) and $\kappa = (2m_N E_B/\hbar^2)^{1/2}$, where E_B is the three-cluster separation energy and m_N the nucleon mass. Since we are interested in the $\alpha(nn)$ relative motion, ϱ can be expressed as $\varrho = \sqrt{\frac{4}{3}\rho^2_{\alpha(nn)} + \frac{1}{2}\rho^2_{nn}}$. We checked that our $\chi^{\alpha(nn)}_{0[00]0}$ relative motion function satisfies the asymptotic form (10) (the other channels only slightly contribute when ρ_{nn} is small and $\rho_{\alpha(nn)}$ is large).

Finally, to test the contribution coming from the halo part of the ^{6}He wave function, we choose to expand the $\rho_{\alpha(nn)}$ space in (5) with 10 basis functions which cover only the 0–10 fm region. Of course this truncation does not affect the ^{6}He energy. The corresponding asymptotic behavior of $\chi^{\alpha(nn)}_{0[00]0}$ is also shown in Fig. 3. The resulting dW/dE is the short-dashed curve in Fig. 2. As we can see, neglecting the $8 - 10 < \rho_{\alpha(nn)} < 25$ fm part of the ^{6}He wave function can cause an order of magnitude error. This confirms that the branching ratio is very sensitive to the halo part of the ^{6}He wave function, as was pointed out in Ref. [12].

The theoretical curve displays a satisfactory order of magnitude although the data appear to be underestimated by about a factor 1.7 between 0.6 and 1.45 MeV. Its shape resembles the experimental curve, but translated by about 200 keV toward lower energies. As such a translation does not have any obvious theoretical explanation, let us first discuss to which extent experiment constrains the shape of the theoretical curve. The data curve is significant only between 0.6 and 1.45 MeV. Below this region, the experimental cutoff hides the energy dependence of the results. Very few events (five) are observed above 1.45 MeV. Hence the real shape of dW/dE and in particular the location of its maximum remain open questions. As we now discuss, these questions are of theoretical importance.

Most theoretical results (those of the present microscopic calculation and of its two approximations displayed in Fig. 2, those of Refs. [10,11], and several cases studied in Ref. [12]) display a common energy behavior with a maximum between 0.3 and 0.4 fm. Only the magnitude of dW/dE varies strongly. Notable exceptions are given by the EH3 and EH results in Ref. [12] whose maximum is at or beyond 0.5 fm, and the EH2 result which displays a zero near 0.6 MeV in contradiction with experiment. These nonstandard shapes follow from small modifications in the external component of the GT matrix element for a fixed internal component. In spite of their apparently better agreement with the available data, the EH3 or EH shapes cannot be considered as confirmed. Experimental data below 0.5 MeV (c.m.) would therefore provide information about the nature of the cancellation mechanism between the internal and external components of the GT matrix element [12]. They would discriminate between "standard" curves with similar shapes but varying magnitudes, and "nonstandard" ones with a maximum at larger energies which is compatible with—but not established by—the presently available data. The standard shape is well reproduced by the present microscopic calculation. The 1.7 multiplicative factor might partly be due to the difficulty of determining the absolute normalization of experiment. The nonstandard shapes require a very specific cancellation mechanism and would indicate the need for further improvements of the theory.

The discrepancy between theory and experiment for dW/dE can possibly be attributed to the same mechanism as the few-percent discrepancy in $B_{\rm GT}$(g.s.). A rather small correction acting mainly on the internal part of the matrix element which would provide a correct $B_{\rm GT}$(g.s.) should modify much more strongly dW/dE and might even affect its energy dependence. A good candidate is provided by meson-exchange currents. Indeed meson-exchange corrections might have the necessary order of magnitude and should affect differently the internal and external parts of the GT matrix elements since the distances between the subsystems are different. Rather small modifications of the internal part may result in 50–100% modifications in dW/dE as discussed in Ref. [12], and as shown here by the test calculation. The fact that the tensor force is not taken into account in the description of the $\alpha + d$ scattering may also play some role, but is probably less important than for the ^{6}Li ground state. Its introduction in the model would, however, exclude the use of the Minnesota force and require the difficult construction of a new force satisfying conditions (i)–(vi) of Sec. I.

IV. CONCLUSION

In summary, we have studied the β delayed deuteron emission from ^{6}He in a microscopic cluster model. We have chosen the Minnesota nucleon-nucleon interaction which reproduces the bulk properties of the free clusters and gives a very good agreement with the experimental $N + N$ and $\alpha + N$ phase shifts in all relevant partial waves. This interaction was shown to provide a good overall description of the ground state of ^{6}He [7]. In the present work we point out that this interaction also provides high quality results for the ground state and $\alpha + d$ scattering states of ^{6}Li. All these results are obtained

without any free parameter. The ^{6}He, ^{6}Li, and $\alpha + d$ wave functions are used to calculate the Gamow-Teller matrix element of the β decay process.

In a calculation of the transition to the ^{6}Li ground state we emphasize the importance of using a consistent description for the systems appearing in the initial and final states, respectively. The results for the β decay toward continuum states show the strong sensitivity to the halo part of the ^{6}He wave function predicted in Ref. [12]. Our best model gives a β delayed deuteron spectrum close to the experiment: The branching ratio is 3.1×10^{-6} to be compared with $(7.6 \pm 0.6) \times 10^{-6}$ [9], when the experimental cutoff is assumed. The total theoretical branching ratio is 6.0×10^{-6}. We argue that the difference between the theoretical and experimental dW/dE has the same origin as the small difference between the values for B_{GT}(g.s.) in spite of the fact that it is much larger. We conjecture that corrections due to meson-exchange currents are important enough to explain these differences.

ACKNOWLEDGMENTS

A. C. was supported by the Science Policy Office (Belgium) and by OTKA Grants Nos. 3010 and F4348 (Hungary). He is grateful to the members of the Theoretical Nuclear Physics Department of the Université Libre de Bruxelles for their kind hospitality, and to M. Kruglanski for his help.

[1] I. Tanihata, H. Hamagaki, O. Hashimoto, Y. Shida, N. Yoshikawa, K. Sugimoto, O. Yamakawa, T. Kobayashi, and N. Takahashi, Phys. Rev. Lett. **55**, 2676 (1985).

[2] P. G. Hansen and B. Jonson, Europhys. Lett. **4**, 409 (1987); P. G. Hansen, Nucl. Phys. **A553**, 89c (1993).

[3] M. V. Zhukov, B. V. Danilin, D. V. Fedorov, J. M. Bang, I. J. Thompson, and J. S. Vaagen, Phys. Rep. **231**, 151 (1993).

[4] V. I. Kukulin, V. M. Krasnopol'sky, V. T. Voronchev, and P. B. Sazonov, Nucl. Phys. **A453**, 365 (1986).

[5] D. R. Lehman and W. C. Parke, Phys. Rev. C **28**, 364 (1983); W. C. Parke and D. R. Lehman, *ibid.* **29**, 2319 (1984).

[6] Y. Suzuki, Nucl. Phys. **A528**, 395 (1991).

[7] A. Csótó, Phys. Rev. C **48**, 165 (1993).

[8] K. Riisager, M. J. G. Borge, H. Gabelmann, P. G. Hansen, L. Johannsen, B. Jonson, W. Kurcewicz, G. Nyman, A. Richter, O. Tengblad, and K. Wilhelmsen, Phys. Lett. B **235**, 30 (1990).

[9] M. J. G. Borge, L. Johannsen, B. Jonson, T. Nilsson, G. Nyman, K. Riisager, O. Tengblad, and K. Wilhelmsen Rolander, Nucl. Phys. **A560**, 664 (1993).

[10] P. Descouvemont and C. Leclercq-Willain, J. Phys. G **18**, L99 (1992).

[11] M. V. Zhukov, B. V. Danilin, L. V. Grigorenko, and N. B. Shul'gina, Phys. Rev. C **47**, 2937 (1993).

[12] D. Baye, Y. Suzuki, and P. Descouvemont, Prog. Theor. Phys. **91**, 2 (1994).

[13] D. R. Thompson, M. LeMere, and Y. C. Tang, Nucl. Phys. **A268**, 53 (1977); I. Reichstein and Y. C. Tang, *ibid.* **A158**, 529 (1970).

[14] Y. Fujiwara and Y.C. Tang, Phys. Rev. C **43**, 96 (1991); Few-Body Systems **12**, 21 (1992).

[15] D. Baye and P. Descouvemont, Nucl. Phys. **A481**, 445 (1988).

[16] P. N. Shen, Y. C. Tang, Y. Fujiwara, and H. Kanada, Phys. Rev. C **31**, 2001 (1985).

[17] M. Kamimura, Prog. Theor. Phys. Suppl. **68**, 236 (1980).

[18] J. L. Friar, G. L. Payne, V. G. J. Stoks, and J. J. de Swart, Phys. Lett. B **311**, 4 (1993).

[19] A. Csótó and R. G. Lovas, Phys. Rev. C **46**, 576 (1992).

[20] L. C. McIntyre and W. Haeberli, Nucl. Phys. **A91**, 382 (1967); B. Jenney, W. Grüebler, V. König, P. A. Schmelzbach, and C. Schweizer, *ibid.* **A397**, 61 (1983).

[21] V. I. Kukulin, V. G. Neudatchin, I. T. Obukhovski, and Yu. F. Smirnov, in *Clusters and Subsystems in Light Nuclei*, edited by K. Wildermuth and P. Kramer (Vieweg, Braunschweig, 1982).

[22] D. Baye, P. Descouvemont, and M. Kruglanski, Nucl. Phys. **A550**, 250 (1992).

[23] F. Ajzenberg-Selove, Nucl. Phys. **A490**, 1 (1988).

[24] J. Carlson, D. O. Riska, R. Schiavilla, and R. B. Wiringa, Phys. Rev. C **44**, 619 (1991).

[25] S. P. Merkur'ev, Yad. Fiz. **19**, 447 (1974) [Sov. J. Nucl. Phys. **19**, 222 (1974)].